Spatiotemporal Frequency Responses of Cat Retinal Ganglion Cells

L. J. FRISHMAN, A. W. FREEMAN, J. B. TROY, D. E. SCHWEITZER-TONG, and C. ENROTH-CUGELL

From the Departments of Neurobiology and Physiology and of Engineering Sciences and Applied Mathematics, Northwestern University, Evanston, Illinois 60201

ABSTRACT Spatiotemporal frequency responses were measured at different levels of light adaptation for cat X and Y retinal ganglion cells. Stationary sinusoidal luminance gratings whose contrast was modulated sinusoidally in time or drifting gratings were used as stimuli. Under photopic illumination, when the spatial frequency was held constant at or above its optimum value, an X cell's responsivity was essentially constant as the temporal frequency was changed from 1.5 to 30 Hz. At lower temporal frequencies, responsivity rolled off gradually, and at higher ones it rolled off rapidly. In contrast, when the spatial frequency was held constant at a low value, an X cell's responsivity increased continuously with temporal frequency from a very low value at 0.1 Hz to substantial values at temporal frequencies higher than 30 Hz, from which responsivity rolled off again. Thus, 0 cycles·deg^{-1} became the optimal spatial frequency above 30 Hz. For Y cells under photopic illumination, the spatiotemporal interaction was even more complex. When the spatial frequency was held constant at or above its optimal value, the temporal frequency range over which responsivity was constant was shorter than that of X cells. At lower spatial frequencies, this range was not appreciably different. As for X cells, 0 cycles·deg^{-1} was the optimal spatial frequency above 30 Hz. Temporal resolution (defined as the high temporal frequency at which responsivity had fallen to 10 impulses·s^{-1}) for a uniform field was ~95 Hz for X cells and ~120 Hz for Y cells under photopic illumination. Temporal resolution was lower at lower adaptation levels. The results were interpreted in terms of a Gaussian center-surround model. For X cells, the surround and center strengths were nearly equal at low and moderate temporal frequencies, but the surround strength exceeded the center strength above 30 Hz. Thus, the response to a spatially uniform stimulus at high temporal frequencies was dominated by the surround. In addition, at temporal frequencies above 30 Hz, the center radius increased.

INTRODUCTION

Spatial frequency responses of cat retinal ganglion cells having center-surround receptive fields have been reported in several studies (e.g., Enroth-Cugell and

Address reprint requests to Dr. Laura J. Frishman, Dept. of Physiology, S-762, University of California, San Francisco, San Francisco, CA 94143-0444. Dr. Freeman's present address is Dept. of Physiology, F13, University of Sydney, New South Wales 2006, Australia.

J. GEN. PHYSIOL. © The Rockefeller University Press · 0022-1295/87/04/0599/30 $1.00

Volume 89 April 1987 599–628

Robson, 1966; Derrington and Lennie, 1982; Linsenmeier et al., 1982; Enroth-Cugell et al., 1983; Dawis et al., 1984). In some studies (Enroth-Cugell and Robson, 1966; Linsenmeier et al., 1982), spatial frequency responses were measured only for relatively low temporal frequencies (2–4 Hz), and it was found that, under these conditions, Rodieck's (1965) difference-of-Gaussians model of the receptive field satisfactorily accounted for the responses. In Rodieck's model, both the center and surround mechanisms of the receptive field are assumed to have Gaussian spatial distributions of sensitivity to light, with the surround having a greater spatial spread: the output of the cell is modeled as the scalar difference of signals from the center and surround mechanisms.

While the difference-of-Gaussians model provides an adequate prediction of the spatial frequency responses of X retinal ganglion cells for contrast modulated at low temporal frequencies, Enroth-Cugell et al. (1983) have shown that the model must be revised to account for their responses to contrast modulated at higher temporal frequencies. In particular, they showed that in order to model the spatial frequency responses of X cells to sinusoidal luminance gratings whose contrasts were modulated at a range of temporal frequencies (0.5–32 Hz), vector addition of signals from the center and surround mechanisms was needed. This model will be referred to as the Gaussian center-surround model.

We have now extended the investigation of the spatiotemporal frequency responses of X and Y cells to temporal frequencies beyond 32 Hz. For X cells, data from photopic, midmesopic, and high scotopic adaptation levels are included, and the usefulness of the Gaussian center-surround model as a description of photopic X cell responses at temporal frequencies up to 90 Hz has been evaluated.

METHODS

Our methods for optic tract and intraocular recordings from cats have been described in detail elsewhere (Enroth-Cugell et al., 1980, 1983) and will be reviewed only briefly here. Surgical anesthesia was induced either with halothane or ketamine hydrochloride and followed during surgery by thiamylal sodium. Atropine sulfate was injected to minimize salivation caused by the anesthestics, and dexamethasone was administered to inhibit inflammatory reactions. During recording, anesthesia was maintained with ethyl carbamate and paralysis was maintained with gallamine triethiodide. The expired CO_2, mean arterial blood pressure, and heart rate were kept at normal levels. The subscapular temperature was held between 38 and 39°C.

After local application of atropine and phenylephrine hydrochloride, contact lenses with 4-mm-diam pupils were fitted to the eyes. The lens power required to bring the stimulus pattern into focus on the retina was determined by direct ophthalmoscopy and, in later experiments, by bringing the vessels around the area centralis into good focus using the illumination technique of Pettigrew et al. (1979). During the experiments, this refraction was tested and corrected if necessary with spherical spectacle lenses to obtain the best possible spatial resolution from X cells with receptive fields in the most central retinal locations.

Recording

Extracellular action potentials from single cells were recorded either from the optic tract with tungsten microelectrodes (Levick, 1972) or from the retinal surface with micropi-

pettes. The micropipettes were filled with 3 M NaCl and thick-slurry beveled (Lederer et al., 1979) to an impedance of 10 MΩ at 60 Hz.

Visual Stimulation

The cats faced a tangent screen with a mean luminance of ~20 $cd \cdot m^{-2}$, and images of the optic disk and other retinal landmarks were projected onto it and traced there (Pettigrew et al., 1979). Light spots or black and white cardboard wands were used against this background to locate the centers of the receptive fields; the locations were then marked on the tangent screen. All subsequent visual stimulation of the cell was performed with patterns presented on the screen of a cathode ray tube (Joyce Electronics, Cambridge, England).

The display subtended 31° × 22° as viewed with a mirror, and had a frame rate of 200 Hz in a few early experiments and 250 Hz in later ones. The mean luminance of the screen was fixed, for each experiment, at a luminance between 200 and 440 $cd \cdot m^{-2}$; lower luminances were obtained by placing calibrated neutral density filters in front of the screen. Stimulus patterns were of constant luminance in the vertical direction, with luminance modulated in the horizontal direction to form an edge or a sinusoidal grating. The contrast of these patterns is defined as the difference between maximum and minimum luminances divided by their sum. The patterns were either stationary, with contrast modulated sinusoidally over time, or they drifted across the receptive field of a cell. Regardless of the contrast, spatial configuration, or mode of modulation of the stimulus, the space- and time-averaged luminance of the screen remained constant. The entire visual stimulation and data collection system was checked with an electronic device that simulates a retinal X cell center response (Schweitzer-Tong, 1983).

Response Measurement

Whether the stimulus was stationary, with contrast modulated sinusoidally in time, or drifting, the amplitude of the cell's discharge rate was measured at the temporal frequency of stimulation (the fundamental Fourier component of the response) and at twice that frequency (the second harmonic). For the fundamental component, the temporal phase angle of the response relative to the stimulus was also determined. Fourier analysis was performed over the integral number of periods of the stimulus that fell within trials of 10.24 s when the frame rate of the stimulator was driven by the computer at 200 Hz, and trials of 8.19 s when it was driven at 250 Hz. The occurrence times of impulses were measured to the nearest 5 ms when 200 Hz was used, and to the nearest 4 ms when 250 Hz was used. When stimulus conditions were altered, responses were not collected until a steady state had been reached.

It is appropriate to state precisely how the terms relating to response are to be used throughout this article. "Frequency response" refers to the fundamental Fourier component of a cell's discharge normalized with regard to contrast. Its magnitude, termed "responsivity" (Enroth-Cugell et al., 1983), is the amplitude of the fundamental Fourier component divided by the contrast of the stimulus that elicited the response. Its phase is referenced to the temporal phase of the stimulus and is given in degrees. The response phase is positive when the response leads the stimulus and is negative when the response lags the stimulus.

Experimental Protocol

In this article, we deal only with X and Y retinal ganglion cells (Enroth-Cugell and Robson, 1966), which presumably correspond to the brisk-sustained and brisk-transient cells, respectively, of Cleland and Levick (1974). When a unit was first isolated, the type of

center, on or off, was determined, and the position of the center was marked on the tangent screen. Then the mirror was adjusted so that the projection of the center of the receptive field was aligned with the middle of the cathode ray tube screen. Precise horizontal positioning was accomplished by rotating the mirror to null the fundamental component of the unit's discharge in response to sinusoidal modulation of the contrast of an edge centered on the screen. This position served as an origin for the horizontal location of the gratings. X and Y cells were differentiated by the "modified null test" (Hochstein and Shapley, 1976).

All spatial and temporal frequency response measurements were made for mean-to-peak amplitudes of the fundamental between 8 and 16 impulses·s^{-1}. A minimum of 20.48 s of discharge was used for each measurement.

The Gaussian Center-Surround Model

Rodieck (1965) introduced the difference-of-Gaussians model for the receptive fields of cat retinal ganglion cells and used it to simulate successfully responses to spot and bar stimuli. Enroth-Cugell and Robson (1966) employed the same model to interpret an X cell's response to gratings drifting across its receptive fields at a fixed low temporal frequency. The model assumes separability of spatial and temporal parameters of the receptive field. Later, Enroth-Cugell et al. (1983) found that in order to account for responses measured at temporal frequencies up to 16 or 32 Hz, some spatiotemporal interaction had to be incorporated into the model. They achieved this by assuming that the signal caused by the surround mechanism was delayed a few milliseconds relative to that caused by the center mechanism. This surround-center delay could be incorporated either via a transport delay or by a single-stage low-pass filter with a time constant of a few milliseconds. Either formulation of the Gaussian center-surround model adequately predicted X ganglion cell responses for all spatial frequencies at temporal frequencies in the range 1–16 Hz. In both formulations, Enroth-Cugell et al. assumed that the ratio of surround to center strength did not change with temporal frequency. We have now observed that a model that fixes the ratio of center to surround strength does not adequately describe the response of X cells to higher temporal frequencies. This can be seen by comparing the predicted ratio of surround to center strength in Fig. 8*A* of Enroth-Cugell et al. with the results of our decompositions of frequency responses into center and surround components in Figs. 11 and 12.

Although a model with the precise temporal characteristics for center and surround mechanisms proposed by Enroth-Cugell et al. (1983) is inadequate to describe our data, we were interested to assess the usefulness of the Gaussian center-surround model in a more general framework. As in all previous models, we assume the X cell receptive field to be a linear, stable, and time-invariant system. The input to the model is a space- and time-varying luminance pattern; the response, which is the time-varying impulse rate of a ganglion cell, is assumed to result from the vector sum of signals from the center and surround components. Since all the spatial stimuli used to measure frequency responses in this study were gratings for which luminance varied in only one spatial dimension, the spatiotemporal frequency response can be represented as:

$$R_g(u, w) = R_c(u, w) + R_s(u, w), \tag{1}$$

where u is spatial frequency, w is temporal frequency, and R_c and R_s are the spatiotemporal frequency responses of the center and surround mechanisms, respectively. Modulation of the luminance at any point in the stimulus was a sinusoidal function of time, so that the response and its components were also temporal sinusoids of the same frequency. As such, they have both amplitude and phase, and can be presented in complex polar notation:

$$|R_g(u, w)|e^{iP_g(u,w)} = |R_c(u, w)|e^{iP_c(u,w)} + |R_s(u, w)|e^{iP_s(u,w)}, \quad (2)$$

where $i = \sqrt{-1}$, the fences represent absolute magnitude, and P_g, P_c, and P_s are the response phases of the cell, its center, and its surround mechanisms, respectively.

It is assumed that the spatial distributions perpendicular to the grating bars of the responsivity of the center and surround components are Gaussian, with coincident peaks but different spatial extents. Further, the phases of the center and surround signals are assumed to be independent of the spatial frequency:

$$|R_g(u, w)|e^{iP_g(u,w)} = S_c(w)e^{iP_c(w)-[\pi u r_c(w)]^2} + S_s(w)e^{iP_s(w)-[\pi u r_s(w)]^2}, \quad (3)$$

where

$$S_c(w) = |R_c(0, w)| \text{ and } S_s(w) = |R_s(0, w)|$$

represent the center and surround responsivities to a spatially uniform field (i.e., the center and surround strengths), and $r_c(w)$ and $r_s(w)$ are the radii of the center and surround spatial responsivity distributions and are assumed here to vary with temporal frequency.

Fitting the Model to Experimental Data

The model has six parameters at each temporal frequency: center and surround radii, center and surround strengths, and center and surround phases. To find the best-fitting parameters for a data sample from an individual cell, the values of these parameters were chosen to minimize the sum of squared errors. The error value used for each measurement of the cell's response was the magnitude of the difference between the experimental and model frequency responses divided by the cell's responsivity (since the responsivity was shown by Enroth-Cugell et al., 1983, to be proportional to the standard deviation of the measurement). The best fit was obtained by a fine and complete search of the whole error surface for plausible values of center and surround radii.

RESULTS

Our major goal was to characterize the spatiotemporal frequency responses of X and Y retinal ganglion cells. We sampled the spatiotemporal frequency response surface quite coarsely in terms of spatial frequency but finely in terms of temporal frequency. We chose three spatial frequencies for each cell, as described below. For each of these spatial frequencies, we measured temporal frequency responses at octave steps from 0.1 to ~25 Hz and at every 4 Hz for higher temporal frequencies. In all cells, we measured spatial frequency responses at 2 Hz at octave or smaller steps for spatial frequencies in the range 0.01 cycles·deg^{-1} to a spatial frequency beyond that for which responsivity was maximal. In some X cells, we also measured spatial frequency responses in similar steps at higher temporal frequencies. We feel that, together with the results of the earlier study by Enroth-Cugell et al. (1983) of X cell spatiotemporal frequency responses in the range 0.5–32 Hz, a detailed description of the photopic spatiotemporal frequency response surface for X cells has now been obtained. We present data from 36 X and 7 Y cells from 17 cats. The receptive fields of the X cells were located between 1° and 34° from the area centralis; 24 X cells were within the central 10°. The receptive fields of the Y cells lay between 3° and 36° from the area centralis; four were within the central 10°.

Choices of Spatial Stimuli

For each cell, X or Y, we measured first the spatial frequency response with sinusoidal gratings drifting at 2 Hz. The resulting curve was used to select three spatial frequencies, as illustrated in Fig. 1. The first was the frequency that maximized the cell's responsivity, which will be referred to as the "peak" stimulus. It should be noted that, as will be shown, the peak stimulus is not a cell's optimal spatial frequency at all temporal frequencies. The second, the "center" stimulus, was selected from the high-frequency limb of the curve at a spatial frequency for

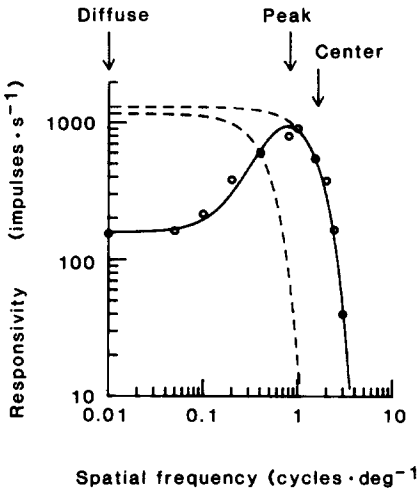

FIGURE 1. Method for choosing stimulus spatial frequencies. The circles show responsivities for an on-center X cell (13X8) as a function of the spatial frequency of gratings drifting at 2 Hz. (Responsivity is the amplitude of the fundamental Fourier component of the impulse rate divided by the stimulus contrast.) The continuous curve is the best fit of the Gaussian center-surround model described in the Methods. The dashed curves show the responsivities of the center and surround components of the model. The "diffuse" stimulus was a grating with a spatial frequency of 0.01 cycles·deg^{-1}, the "peak" stimulus had a spatial frequency that maximized responsivity, and the "center" had a spatial frequency that was chosen to give a responsivity between two and four times less than that with the peak stimulus. The mean luminance of the screen was 340 cd·m^{-2}, and the cat had a 4-mm-diam artificial pupil.

which the cell's responsivity was two to four times below maximum. It has previously been shown that, at these high spatial frequencies, the cell's response is essentially due to its center signal alone (e.g., Enroth-Cugell and Robson, 1966; Linsenmeier et al., 1982). This can be seen in Fig. 1, where the dashed curves represent the relative contributions to the cell's response of center and surround components as a function of spatial frequency. The third, the "diffuse" stimulus, maximized the signals from both the center and the surround. We used either a uniform field that filled the entire screen of the stimulator and whose luminance was modulated sinusoidally in time or a drifting 0.01 cycles·deg^{-1} grating.

Drifting and stationary grating stimuli of the same spatial frequency yielded the same frequency response measurements.

Photopic Spatiotemporal Frequency Responses

Photopic spatiotemporal frequency responses for an on-center X cell are shown in Fig. 2. Except for a vertical displacement in responsivity, the temporal

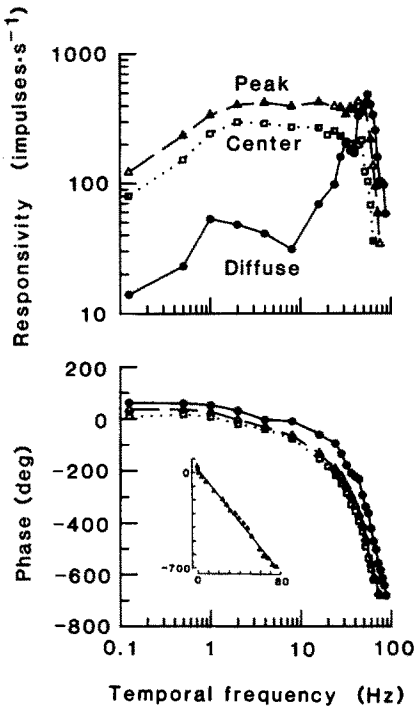

FIGURE 2. Photopic spatiotemporal frequency response of an on-center X cell. The upper plot shows the responsivity of an X cell (10X3) stimulated with diffuse (0.01 cycles·deg^{-1}, circles), peak (1.4 cycles·deg^{-1}, triangles), and center (2.4 cycles·deg^{-1}, squares) spatial frequencies drifted at a range of temporal frequencies. The lower plot shows the corresponding phase data in degress of phase advance relative to the stimulus. In this figure as well as in Figs. 3, 4, and 6, the lines simply connect the data points and do not represent a fitted model. The inset in the lower plot shows the phase data for the peak stimulus plotted on linear-linear axes and the straight line is a linear regression fit to these data. The mean luminance of the screen was 340 cd·m^{-2}.

frequency responses for peak and center stimuli were quite similar. Typical of the X cells we studied, responsivity changed little over a considerable range of temporal frequencies. This is evident from estimates of bandwidth, which can be read from the curves as the frequency difference in octaves between the upper and lower frequencies for which responsivity has declined 3 dB from maximum. For the peak stimulus, the 3-dB range was from 0.5 to 16 Hz

(bandwidth, 5 octaves) and, for the center stimulus, it was from 1 to 28 Hz (bandwidth, 4.8 octaves). The average ranges for the 17 X cells for which we measured curves with the peak stimulus and the 18 X cells for which we measured curves with the center stimulus are given in Table I. The frequencies at the logarithmic midpoints of these ranges are also given. Clearly, these measurements differed little for peak and center stimuli. The relationship between the response phase and the temporal frequency measured with these two stimuli was also similar. For all stimuli, the response phase was a linear function of the temporal frequency at midrange to high temporal frequencies (see inset). The phase gradient can be used as a measure of the cell's visual latency. If the system being studied acted as a pure delay, its responsivity would not vary with temporal frequency, and its phase would be proportional to temporal frequency. The frequency range over which the response conformed to these requirements was sufficiently wide that the interpretation of the phase gradient as a latency is a useful one. With the peak stimulus, the slope of this relationship was -9.8 deg·Hz^{-1}, i.e., a latency of 27.2 ms. The average latency is given in the table.

In order to quantify the response attenuation seen at temporal frequencies above and below the 3-dB range, we measured the slopes on double-logarithmic axes of the relationships between responsivity and temporal frequency for the range 0.1–1.0 Hz and of the high-frequency limb. The roll-off was much shallower at low frequencies. Although, for the cell whose frequency responses are illustrated in Fig. 2, the slope was similar for peak and center stimuli (0.48 and 0.52, respectively), for the entire sample it was a little steeper for the peak stimulus, as shown in Table I. At the high-frequency end, the slopes were in the range -6 to -8 for both spatial patterns.

The responsivity for the diffuse stimulus was much smaller than that for the peak stimulus over a broad range of temporal frequencies. In addition, between 0.1 and 1 Hz, the roll-off in responsivity was steeper than for the other spatial patterns. For the cell illustrated in Fig. 2, the slope on double-logarithmic coordinates was 0.6. An average value for the slope with the diffuse stimulus could not be reported in the table, however, since for most cells responsivities were so low at temporal frequencies of <0.5 Hz that we had insufficient data points (see Fig. 3) to quantify the roll-off. This strong attenuation of the responses of X cells to diffuse stimuli under photopic conditions has been noted previously (Derrington and Lennie, 1982).

The responsivities measured for the diffuse stimulus displayed an interesting dependence on the temporal frequency around and past 40 Hz that was also evident, but to a much lesser extent, in the curves measured with the peak and center stimuli. A small dip in responsivity occurred near 40 Hz, followed by a marked increase in responsivity. As a result of this increase, the diffuse stimulus became the cell's optimal stimulus at some high temporal frequency and remained so for all higher temporal frequencies. The response phase for the diffuse stimulus led those for peak and center stimuli at all temporal frequencies. These features of the temporal frequency response of X cells measured for diffuse stimuli were observed first in the course of the study reported in Enroth-Cugell et al. (1983).

TABLE I

Summary of the Characteristics of X and Y Retinal Ganglion Cell Frequency Responses

Cell type	Adaptation level	Spatial stimulus	Slope of low temporal frequency roll-off	3-dB range			Slope of high temporal frequency roll-off	Temporal resolution	Slope of phase curve
				Low end	High end	Logarithmic midpoint, high and low end			
				Hz	*Hz*	*Hz*		*Hz*	*ms*
X	Photopic	Diffuse		33.60 (17.4)	58.00 (24.0)	40.8 (19.2) [19]*	−7.3 (1.1)	94.9 (9.2) [17]	
		Peak	0.55 (0.14) [15]	1.20 (0.6)	30.10 (21.2)	5.6 (2.9) [17]	−8.3 (1.0)	85.6 (7.8) [17]	24.1 (3.7) [17]
		Center	0.42 (0.16) [17]	1.70 (1.3)	27.30 (8.6)	6.3 (2.6) [17]	−6.7 (1.3)	62.6 (9.3) [17]	
	Midmesopic	Diffuse	0.70 (0.24) [9]	6.00 (1.3)	19.70 (3.0)	10.8 (1.5) [9]	−5.1 (0.9)	52.9 (11.1) [9]	
		Peak	0.55 (0.09) [13]	2.10 (2.3)	16.00 (3.6)	5.1 (2.9) [11]	−6.0 (0.9)	41.1 (7.0) [11]	33.4 (4.6) [11]
		Center	0.39 (0.10) [4]	0.50 (0.22)	17.00 (1.4)	2.9 (0.6) [4]	−5.5 (1.1)	24.3 (13.0) [4]	
	High scotopic	Diffuse	0.43 (0.06) [3]	1.17 (0.7)	14.0 (5.6)	3.7 (0.7) [3]	−3.7 (1.0)	30.0 (7.4) [3]	
		Peak	0.32 (0.07) [2]	0.23 (0.12)	7.00 (3.6)	1.2 (0.1) [3]	−3.9 (0.2)	25.0 (4.0) [3]	77.2 (11.7) [3]
		Center	0.28 (0.09) [3]	0.03 (0.15)	4.70 (1.2)	1.2 (0.1) [3]	−2.6 (2.2)	18.0 (4.4) [3]	
Y	Photopic	Diffuse	0.56 (0.21) [4]	14.30 (1.7)	30.00 (25.0)	20.2 (20.9)‡ [4]	−8.1 (0.5)	120.0 (10.0) [3]	
		Peak	0.67 (0.22) [6]	2.30 (1.1)	22.30 (20.2)	5.9 (1.6) [7]	−8.1 (0.7)	102.5 (9.4) [4]	20.0 (3.8) [4]
		Center	0.64 (0.05) [2]	3.70 (2.6)	20.80 (8.0)	8.0 (4.3) [6]	−7.3 (2.3)	79.2 (7.5) [5]	

For each measure, average values and standard deviations (the latter in parentheses) are shown for both X and Y cells at a photopic level of adaptation and for X cells at a mesopic and scotopic level of adaptation. Values are shown for the three different spatial stimuli used: the diffuse, the peak, and the center stimulus. The number of cells for which we could make the measurements are shown in brackets. From left to right, the table shows (*a*) the slope of the frequency response between 0.1 and 1 Hz, (*b*) the low-frequency and (*c*) the high-frequency limit of the 3-dB range, (*d*) the logarithmic midpoint of this 3-dB range, (*e*) the slope of the high-frequency limb of the frequency response curve, (*f*) the temporal resolution of the cell (measured by extrapolating the high-frequency limb of the temporal frequency response to intersect the abscissa at a responsivity of 10 impulses·s^{-1}), and (*g*) for peak curves only, the gradient of the high-frequency limb of the phase curve.

* The number of cells varied because of incomplete curves of high or low temporal frequencies.

‡ There was one very high value.

It may be useful at this stage to consider briefly the whole spatiotemporal frequency response surface of the X cell. From the results we have presented so far and from those of Enroth-Cugell et al. (1983), it appears that there are two maxima on the responsivity surface. One is centered on the peak spatial frequency and at a temporal frequency of ~6 Hz. This is a rather gentle maximum, perhaps more appropriately termed a ridge of maximal sensitivity, with responsivity falling slowly from this point as a function of both logarithmic spatial and logarithmic temporal frequency. The second maximum is centered on zero spatial frequency and at a temporal frequency of ~40 Hz. This is a sharp maximum, particularly in terms of logarithmic temporal frequency.

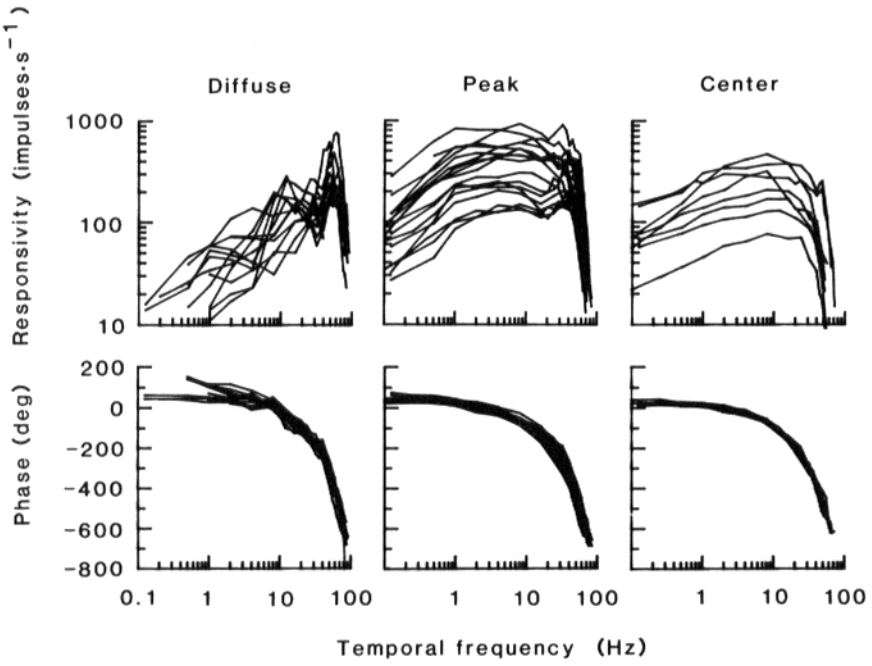

FIGURE 3. Photopic spatiotemporal frequency responses for 17 on-center X cells. Each line in the responsivity plots comes from a single cell and has a corresponding line in the phase plot below it. Measurements are shown as a function of temporal frequency for diffuse, peak, and center stimuli.

The range of variation of the spatiotemporal frequency responses of our X cell sample is illustrated in Fig. 3. Only on-center cells whose temporal frequency response for at least one spatial stimulus was measured over the full range of temporal frequencies are shown. Off-center cells had similar amplitude curves, but their response phases were shifted by 180° from those of on-center cells. Although substantial variation exists in the vertical position of the responsivity curves for each spatial stimulus, their shapes are fairly consistent. A dip in the temporal frequency responsivity between 30 and 40 Hz and an enhanced responsivity at higher temporal frequencies were obvious for the responses of most cells to the diffuse stimulus. The dip was also seen in some of the curves measured

for the peak stimulus, and even in a couple of the curves measured for the center stimulus. The phase curves for each spatial stimulus showed little variation across cells. For the diffuse stimulus, the phase curves tended to show a small kink at about the temporal frequencies for which responsivity dipped. This can be seen in Fig. 2 for cell 10X3; the kink's presence among the population of X cells is obscured by the overlapping of curves in Fig. 3.

Photopic spatiotemporal frequency responses for a representative Y cell are illustrated in Fig. 4. In contrast to the X cells, the fall-off in responsivity for the

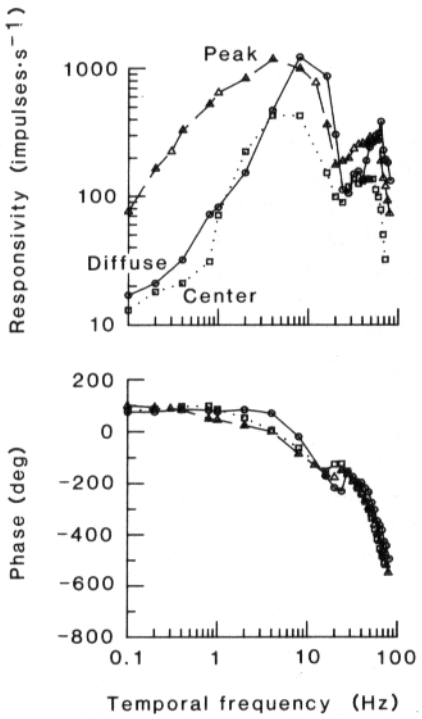

FIGURE 4. Photopic spatiotemporal frequency response for an on-center Y cell (2Y4). Responsivity and phase are shown as a function of the temporal frequency of the drifting stimulus for diffuse (0.01 cycles·deg^{-1}, circles), peak (0.20 cycles·deg^{-1}, triangles), and center (0.42 cycles·deg^{-1}, squares) stimuli. The mean luminance of the screen was 440 cd·m^{-2}.

Y cell at low temporal frequencies was similar for the three spatial stimuli. The average slopes of the relationships between logarithmic responsivity and logarithmic temporal frequency between 0.1 and 1 Hz for center and peak stimuli were steeper for Y cells than for X cells (see Table I).

It is noteworthy that Y cell curves measured with peak and center stimuli revealed a more complex spatiotemporal interaction than those of X cells. The shape of the spatial frequency response of the cell illustrated in Fig. 4 was approximately invariant with temporal frequency up to ~2 Hz. In the range 2–10 Hz, there was a progressive rise in the cell's responsivity to low spatial

frequencies, and from 10 to 20 Hz, "zero" spatial frequency was the optimal stimulus. For another band of temporal frequencies beyond this (20–45 Hz), the peak stimulus was once again optimal. Finally, the diffuse stimulus became optimal once more at even higher temporal frequencies and remained so until the limit of temporal resolution was reached. It appears from Fig. 4 that the spatiotemporal frequency response surface of Y cells has two maxima, as is the case with X cells, but the Y cell maxima are both sharply tuned in terms of logarithmic temporal frequency.

One obvious result of the sharper maxima in the Y cells' temporal frequency response is that their 3-dB ranges were shorter. For the cell illustrated in Fig. 4, the range for the curve measured with the peak stimulus was from 2.2 to 10.4 Hz (bandwidth, 2.2 octaves), and the range for the curve measured with the center stimulus was from 3.7 to 10.8 Hz (bandwidth, 1.5 octaves). The average values for the small sample of Y cells studied are shown in the table. Although the 3-dB ranges for the Y cells were shorter, the logarithmic midpoints of the ranges for the peak and center curves were similar to those of X cells.

As the temporal frequency increased, the amount by which the Y cells' response lagged the stimulus increased, as was the case for X cells. The gradient of the relationship between the response phase and the temporal frequency (on linear axes) for the peak stimulus for the cell in Fig. 4 was -7.7 deg·Hz^{-1} (i.e., 21.4 ms). For Y cells, the kink in the phase curve that occurred around 20 or 30 Hz and corresponded to the dip in the responsivity curve was much more pronounced than it was for X cells.

The slope of the high temporal frequency limb was about the same for Y cells as for X cells, and did not vary appreciably with the choice of stimulus; it was about -8 on double-logarithmic axes for most cells (see Table I for more details). For one Y cell, the spatiotemporal frequency response was more like that measured from X cells.

Photopic Temporal Resolution

We measured temporal resolution by extrapolating the nearly straight high-frequency limbs of the temporal frequency responses to intersect a horizontal line drawn at a responsivity equal to 10 impulses·s^{-1}. The value of the abscissa corresponding to this point of intersection was taken as the high-frequency resolution. This extrapolation is similar to that used by other investigators to estimate spatial resolution from spatial frequency responses (e.g., So and Shapley, 1981; Linsenmeier et al., 1982): it represents the highest temporal frequency at which a sinusoidal grating stimulus of unity contrast can produce a fundamental Fourier component at an amplitude of 10 impulses·s^{-1}.

A source of uncertainty in estimates of temporal resolution for the peak stimulus was that, during a recording session, a cell's peak spatial frequency was not known precisely. In fact, this could only be determined, after a recording session, when the spatial frequency responses measured for contrasts modulated at 2 Hz were fitted with the Gaussian center-surround model. Any error in the spatial frequency selection is reflected in a vertical displacement of the temporal frequency responsivities and a resultant error in the estimate of temporal reso-

lution. Since our errors in selection were always small and we know that the temporal frequency responses are invariant as a function of spatial frequency for spatial frequencies close to the peak spatial frequency, we normalized the temporal frequency responsivities so that, for each cell, the responsivity at 2 Hz was at the maximum predicted by the Gaussian center-surround model. Estimates of temporal resolution with and without this normalization were usually negligibly different, which showed that the frequency selection for the peak stimulus during a recording session had generally been appropriate.

Normalization across cells of the responsivities measured for center stimuli was also performed before temporal resolution was determined. This is again justified by the invariance of the shape of the temporal frequency response with spatial frequency for high spatial frequencies. The 2-Hz responsivity for each cell was normalized to be half the maximum responsivity predicted by the Gaussian center-surround model fitted to the 2-Hz spatial frequency responses. As noted earlier, during the recording sessions, spatial frequencies that yielded responsivities between one-quarter and one-half that of peak responsivity had been selected for the center stimulus. Temporal frequency responses measured for diffuse stimuli required no normalization.

The absolute temporal resolution (obtained with the diffuse stimulus) for X cells ranged from ~80 to 100 Hz. For one Y cell, it was as high as 130 Hz. The average values of temporal resolution for all spatial stimuli are presented in Table I. Having observed that the temporal resolutions for each stimulus form were variable across cells, we were interested to determine the extent to which this variation was systematic. We found a relationship between temporal resolution and the radius of a cell's receptive field center. The center radius is a very useful metric for standardizing ganglion cell properties, since it provides a measure of the spatial scale on which the retinal image is sampled locally (by that class of ganglion cells) and it takes into account (at least for scotopic adaptation levels) the state of light adaptation in that cell (Enroth-Cugell and Shapley, 1973). It is a good metric to use in a retina such as the cat's, where sampling of images is inhomogeneous. However, since the center radius appears to change at high temporal frequencies (see below), it is important that it be determined for all cells at low temporal frequency. It was convenient for us to estimate the center radius from fits of the Gaussian center-surround model to the 2-Hz spatial frequency responses we measured for all cells, and, in Fig. 5, temporal resolution is plotted against this estimate.

Temporal resolutions determined from responses evoked by peak and center stimuli were positively correlated with center radius. The Pearson product moment correlation coefficient for the X cells alone for the curves measured with the peak stimuli was 0.69 ($n = 17$, $p < 0.01$), and for the X and Y cells combined, it was 0.77 ($n = 21$, $p < 0.001$). The correlation coefficient was lower for the curves measured with the center stimuli, 0.44 ($n = 18$, not significant) for X cells, but it was 0.69 ($n = 23$, $p < 0.01$) when all cells were included. Temporal resolution for diffuse stimuli was barely correlated with the receptive field center radius (correlation coefficient, 0.17; $n = 16$) for X cells alone, but when Y cells were included, the correlation was higher (correlation coefficient,

0.63; $n = 19$, $p < 0.01$). Somewhat less strong correlations were observed between temporal resolution and retinal eccentricity in all cases.

In our measurements of temporal resolution described above, we did not attempt to normalize maximum responsivity across cells, assuming rather that it was reasonable (and less biased) to suppose that maximum responsivity might vary from cell to cell. However, an alternative view is that all cells of one class have the same maximum responsivity and that the differences observed within a sample of cells derive from such factors as differences in the physiological state of the animal at the time the measurements were made. Hence, for comparison, we examined temporal resolution when all of the X cell curves measured with center stimuli were normalized to a maximum responsivity of 500 impulses·s^{-1}; the correlation coefficient between resolution and center radius for the X cells was significant (0.48, $n = 18$, $p < 0.05$).

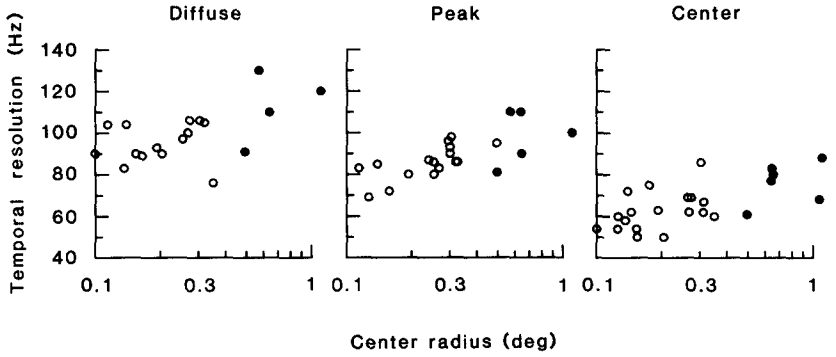

FIGURE 5. Temporal resolutions of X and Y cells at photopic levels of mean retinal illumination. Temporal resolutions were measured by extrapolating the high-frequency limbs of the temporal frequency response; resolution is defined as the temporal frequency at which the responsivity equals 10 impulses·s^{-1}. Resolutions are plotted as a function of the radius of the center mechanism derived from fitting the Gaussian center-surround model to the 2-Hz spatial frequency responses. The open circles represent X cells; the filled circles represent Y cells.

It might be noted, in conclusion, that the high temporal resolution of cat ganglion cells for photopic full-field stimuli requires that experimenters use raster displays with very high refresh rates (≥200 Hz) to study responses from these cells.

Spatiotemporal Frequency Responses at Lower Levels of Retinal Illumination

For some X cells, spatiotemporal frequency responses were measured at levels of mean retinal illumination ~1/100 and 1/10,000 (midmesopic and high scotopic) of the mean photopic levels of the experiments described so far. The spatial frequencies used for diffuse, peak, and center stimuli were the same as those used for photopic levels, except in cases where only the lower levels were studied, and then the spatial stimuli were based on the 2-Hz spatial curves at the midmesopic level. It is relevant to note in passing that, as in previous studies

(Enroth-Cugell et al., 1977; Kirby and Schweitzer-Tong, 1981; Derrington and Lennie, 1982), we found no systematic change in the center radius of the cells' receptive fields as retinal illumination was reduced from photopic to scotopic levels.

For the cell illustrated in Fig. 6, as well as for other cells, the maximum responsivity was hardly altered under midmesopic illumination but was greatly reduced in scotopic illumination. The 3-dB ranges of responsivity for all stimulus configurations were at lower temporal frequencies at mesopic than at photopic levels of illumination, and were lower still under scotopic illumination. The

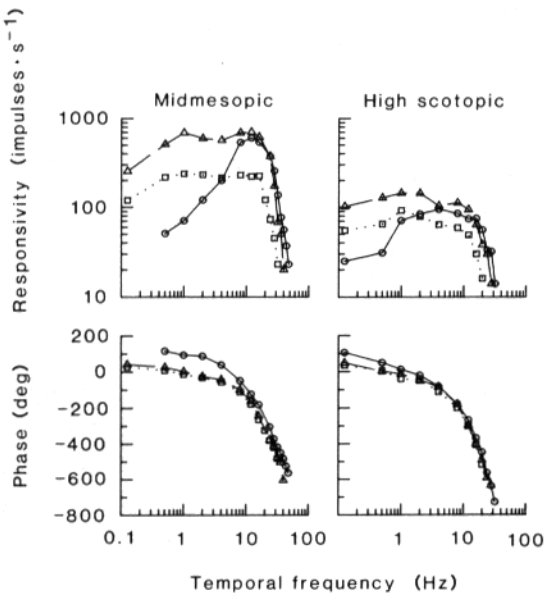

FIGURE 6. X cell spatiotemporal frequency response at lower mean levels of retinal illumination. Spatiotemporal frequency responses for an on-center X cell (11X5) are given for a midmesopic (mean luminance, 2.8 cd·m^{-2}) and a high scotopic (mean luminance, 0.021 cd·m^{-2}) level of light adaptation. Responsivity and phase are shown as a function of temporal frequency for diffuse (0.01 cycles·deg^{-1}, circles), peak (1.22 cycles·deg^{-1}, triangles), and center (2.0 cycles·deg^{-1}, squares) stimuli.

logarithmic midpoints of these ranges were accordingly lower. For instance, for the cell illustrated in Fig. 6, the logarithmic midpoint of the 3-dB range for the peak stimulus was 4.8 Hz under photopic illumination, 3.2 Hz at the mesopic level, and 1.4 Hz at the scotopic level. The average values for all the cells are given in the table. Under mesopic and scotopic illumination, the responsivity for low temporal frequencies of modulation was attenuated with the diffuse stimulus more than with either the peak or center stimuli. Further, higher temporal frequencies were still resolved better with the diffuse stimulus; however, the responsivity and phase functions were smoother than they were for photopic adaptation.

Both temporal resolution and the slope of the high-frequency limb of the responsivity curve were lower at these lower levels of mean illumination for all three spatial stimuli. Fig. 7 illustrates the relationship between temporal resolution and the center radius for the peak stimulus at all three adaptation levels. The table shows that, on average, the slope of the high temporal frequency roll-off in logarithmic responsivity decreased by about one-third for each 100-fold reduction in mean retinal illumination. Further, for the range of temporal frequencies 0.1–1 Hz, the slope of the relationship between logarithmic temporal frequency and logarithmic responsivity became shallower as the mean illumination was decreased. The relationship between the response phase and temporal frequency was also dependent on adaptation. As documented in the table, for peak curves, the magnitude of the gradient relating phase to temporal frequency

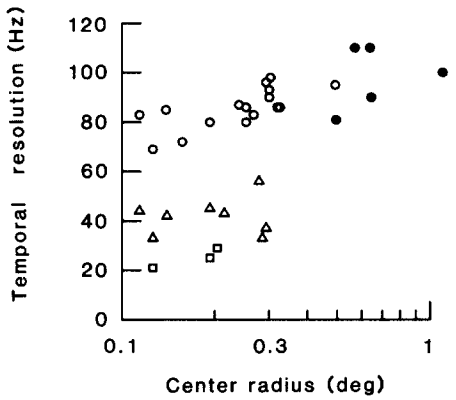

FIGURE 7. X cell temporal resolutions (open symbols) for the peak stimulus at three levels of retinal illumination. Temporal resolution is plotted as a function of center radius at photopic (circles), mesopic (triangles), and scotopic (squares) levels. The radius of the center mechanism is the one determined from the photopic 2-Hz spatial frequency response in most cases. For six units studied only at mesopic levels, the radii were determined from the mesopic 2-Hz spatial frequency response. In cases where the spatial frequency responses were measured at both photopic and mesopic levels, the derived radii were similar. The Y cell photopic resolutions (filled circles) shown in Fig. 5 are included for comparison.

(plotted on linear axes) increased as the adaptation level was decreased. In summary, the responses of X ganglion cells became slower as retinal illumination was reduced. Similar effects of the adaptation level on the temporal frequency response have been reported for cells of the dorsal lateral geniculate nucleus (Kaplan et al., 1979).

Application of the Gaussian Center-Surround Model

The second goal of this study was to interpret the spatiotemporal frequency response of the X cell in terms of the Gaussian center-surround model. Before applying the model to our data, it was first necessary to demonstrate that the model could provide a good fit to spatial frequency responses measured for high temporal frequencies of contrast modulation. To test this, spatial frequency

responses were measured for three on-center X cells at temporal frequencies up to 68 Hz, and the Gaussian center-surround model defined by Eq. 3 was fitted to these data using the procedure outlined in the Methods. The model's six parameters—r_c, S_c, P_c, r_s, S_s, P_s—were allowed to change across temporal frequency. The resulting fits for a representative cell are shown in Fig. 8; the root mean squared error over all points in this figure is 0.179, while the error

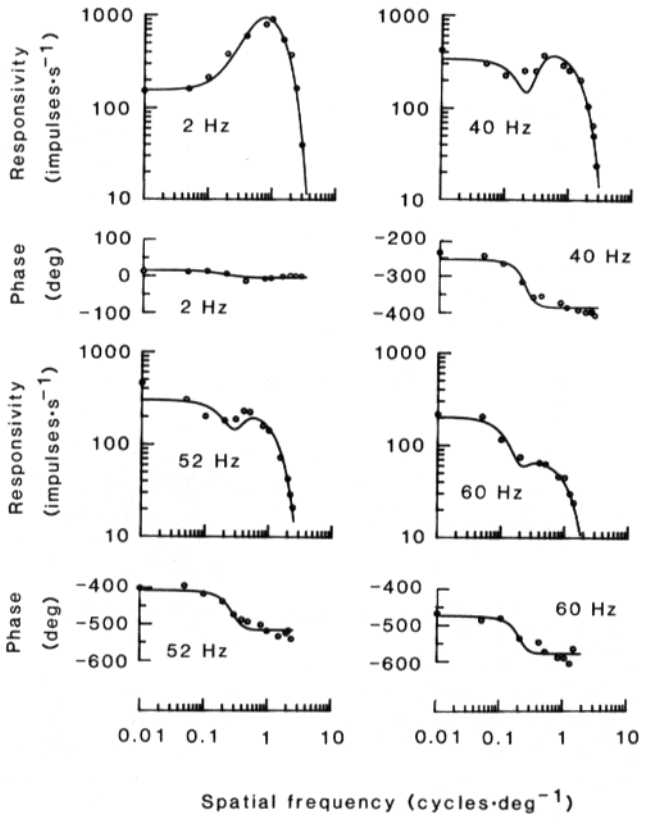

FIGURE 8. X cell photopic spatial frequency responses at four temporal frequencies. Responsivity and phase are plotted as a function of spatial frequency for temporal frequencies of 2, 40, 52, and 60 Hz. Grating patterns were alternately drifted and held stationary with sinusoidal temporal modulation of contrast. Responsivities are based on drifted stimuli; phases are based on stationary stimuli. The continuous curves give the results of fitting the Gaussian center-surround model to the neural data. Same cell (13X8) as in Fig. 1.

over all three cells is 0.182. Although there are discrepancies between the experimental and model data—model responsivity, for instance, is too small at midrange spatial frequencies—the model can reproduce the experimental data from these three cells adequately. Moreover, the error compares favorably with the error over all of the 2-Hz spatial frequency responses that we have fitted.

The center and surround radii used to fit the Gaussian center-surround model

to the data collected for the three on-center X cells at higher temporal frequencies are shown in Fig. 9. The figure shows how the radius of the Gaussian describing the spatial sensitivity of the center mechanism depends on the temporal frequency. Enroth-Cugell et al. (1983) found that the center radius changed little for frequencies up to 32 Hz, but, as shown in Fig. 9, we found that it increased above this frequency. The radius of the surround showed no clear dependence on temporal frequency.

Decomposition of X Cell Spatiotemporal Frequency Responses into Center and Surround Components

Responsivities at high temporal frequencies were greater with the diffuse stimulus than with the peak and center stimuli. Since this spatial stimulus maximizes the contribution from the surround relative to the center (and absolutely), this result

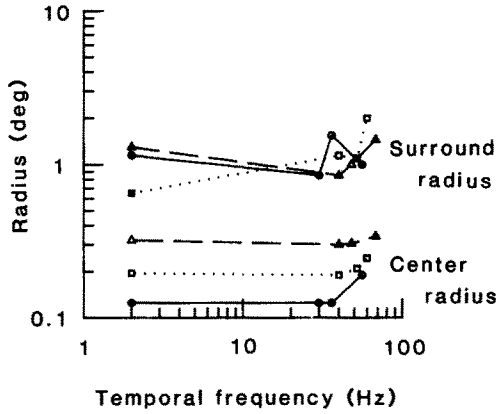

FIGURE 9. Dependence of the radii of center and surround mechanisms on temporal frequency. Photopic spatial frequency responses from the X cell illustrated in Fig. 8 and two other X cells (11X12 and 12X1) were fitted with the Gaussian center-surround model at four temporal frequencies. The resulting center and surround radii are plotted as a function of temporal frequency. Radius estimates from the same cell are connected by lines. The mean luminance was 340 cd·m^{-2} for all cells.

strongly suggests that the surround resolves higher temporal frequencies. Indeed, spatial frequency responses measured at high temporal frequencies and fitted with the Gaussian center-surround model imply that the center strength is reduced more rapidly at high temporal frequencies than is the surround strength. This can be seen by comparing Figs. 10 and 1, which show the center and surround components of the 60-Hz and the 2-Hz spatial frequency responses, respectively, of one on-center X cell. Note that both the center and surround strengths were lower at 60 Hz than at 2 Hz, but that the center strength was reduced by a greater factor. Consistent with this relative change in the strengths of the center and surround mechanisms, Fig. 8 shows a much larger dependence of the response phase on the spatial frequency at high temporal frequencies; this results from the predominance of the surround mechanism at low spatial frequencies.

These suggestions about the behavior of the response mechanisms were corroborated by decomposing, at each temporal frequency, the measured responses of the cell to diffuse and peak stimuli into center and surround components using the Gaussian center-surround model. The rationale for this analysis is as follows. Assume that the center and surround radii are known at the temporal frequency in question; the signal from each mechanism at a given spatial frequency can then be estimated. For instance, the factor by which the

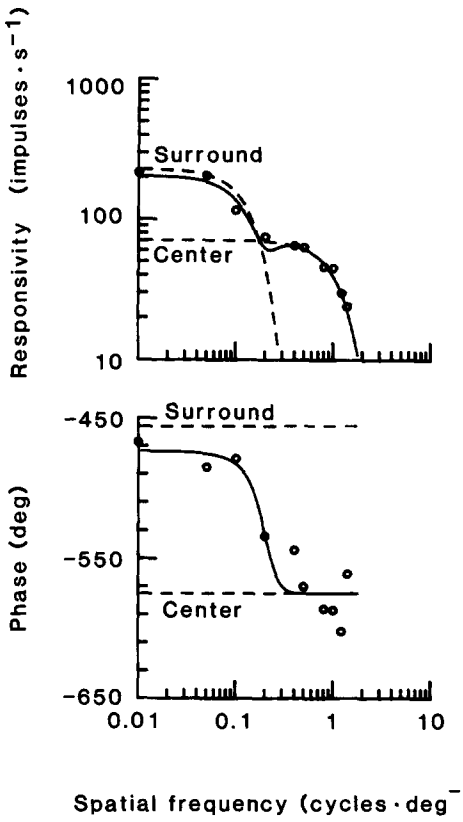

FIGURE 10. Photopic spatial frequency response obtained at 60 Hz and fitted with the Gaussian center-surround model. These data (open circles) are from the cell featured in Figs. 1 and 8. The continuous lines show the fitted Gaussian center-surround model, and the dashed lines show the model center and surround components.

signal from the center evoked by a grating of the peak spatial frequency is attenuated relative to its signal for zero spatial frequency is

$$a_{cp} = e^{-(\pi r_c u_p)^2}, \tag{4}$$

where u_p is the spatial frequency of the peak stimulus. The response to the peak stimulus is largely due to the center, so the center strength (the amplitude of the center's signal at zero spatial frequency) can be approximately determined by

dividing the cell's responsivity to the peak stimulus by a_{cp}; the center phase is essentially equal to the phase of the peak response. (Responses to the peak rather than to the center stimulus were chosen for the decomposition because the responses extended to higher temporal frequencies, thus allowing an analysis over a larger range of frequencies.) The frequency response for the diffuse stimulus is equal, or nearly equal, to the sum of the center and surround signals for zero spatial frequency. The surround signal for zero spatial frequency can be well approximated by the difference between the diffuse frequency response and the center signal.

More rigorously, Eq. 3 and equations for the "attenuation" factors (such as Eq. 4) give the cell's response to the diffuse spatial frequency (u_d):

$$|R_g(u_d)|e^{iP_g(u_d)} = a_{cd}S_c e^{iP_c} + a_{sd}S_s e^{iP_s}, \quad (5)$$

and to the peak stimulus:

$$|R_g(u_p)|e^{iP_g(u_p)} = a_{cp}S_c e^{iP_c} + a_{sp}S_s e^{iP_s}. \quad (6)$$

These are two complex equations that can be split into four real equations, with one equation each for the cosine and sine components of the diffuse and peak responses. Assuming that the spatial parameters r_c and r_s are known, Eqs. 5 and 6 represent four equations that are linear in four unknowns: the cosine and sine components of the center and surround signals. These equations were solved to obtain the center and surround strengths and phases at each temporal frequency used.

Fig. 11 shows the result for the cell whose frequency responses are shown in Fig. 2. The resulting strengths and phases for the center and surround components are shown on the left. The two plots on the right show the ratio of surround to center strength and the difference between the surround and center phases. Fig. 12 illustrates the consistency of these results across 10 on-center units.

The results in Figs. 11 and 12 were generated assuming that the center and surround radii for each cell were fixed at their 2-Hz values. Given the finding illustrated in Fig. 9 that the center radius increases with temporal frequency above ~30 Hz, the consequences of this assumption must be considered. The result of underestimating the center radius is that the amount of attenuation at the peak spatial frequency for the center mechanism and hence the center strength are underestimated. With the center strength underestimated, the surround strength must also be underestimated and the phase of the estimated surround signal will lag the true surround signal. However, since we had measured the spatial frequency responses at high temporal frequencies in three cells and could consequently estimate how the center radius changed as a function of temporal frequency, we were able to determine, for these three cases, the impact of the errors resulting from the assumption of an invariant center radius upon estimates of frequency responses of the center and surround mechanisms. With the data from these cells, we obtained qualitatively similar estimates of the frequency responses of center and surround mechanisms from decompositions of the frequency responses measured for peak and diffuse stimuli made (*a*) with the assumption that the center radius was fixed at its 2-Hz value, and (*b*) with

the center radius allowed to hold its true value at each temporal frequency. Further, the ratio of surround strength to center strength under the first assumption was virtually identical to that under the second, as was the difference between the surround and center phases.

Center and Surround Temporal Frequency Responses

In Fig. 12, the curve for center and surround strengths and phases, obtained by the decomposition just described, is of consistent shape across cells. The strengths of both mechanisms remained approximately constant between 1 and 20 Hz.

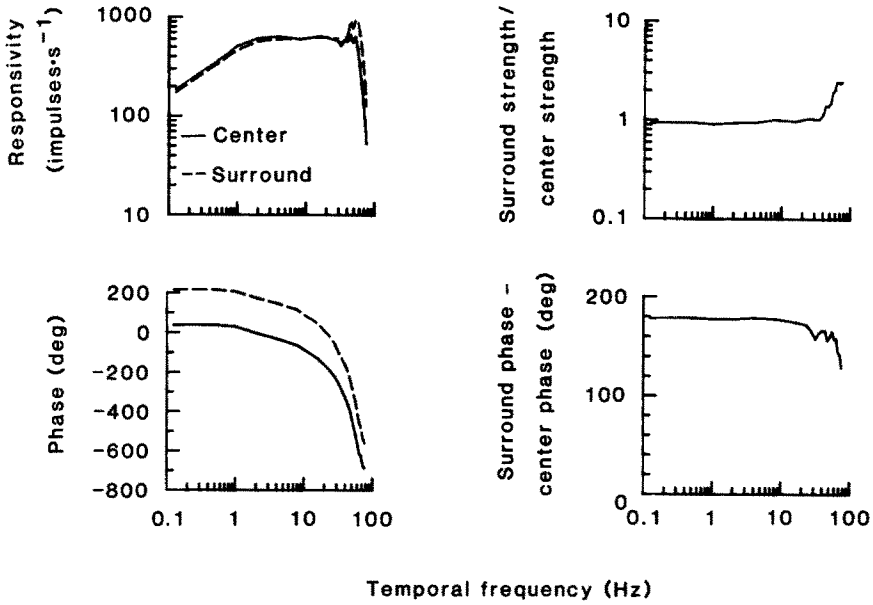

FIGURE 11. Photopic temporal frequency responses for the center and surround mechanisms of an X cell. The responses of an on-center X cell (10X3, same unit as in Fig. 2) to diffuse and peak spatial stimuli were decomposed into center and surround strengths (responsivities at zero spatial frequency) and phases at each temporal frequency used. The curves on the left are the strength and phase of the center (continuous line) and surround (dashed line) mechanisms. On the right, the ratio of surround and center strength and the phase difference between the two mechanisms are shown.

Below 1 Hz, there was a gentle roll-off of ~0.5 log units of strength per log unit of temporal frequency. Above 20 Hz, the strengths of the two mechanisms were different; the surround strength increased to well above the center strength before it dropped. The high-frequency roll-off of the strengths of both mechanisms was rapid, ~6 log units/1 log unit of temporal frequency. Fig. 12 shows that center and surround phases are simple functions of temporal frequency. Both center and surround phase plots are well approximated by linear functions of temporal frequency with a gradient of about -9 deg·Hz^{-1} (i.e., 25 ms). The difference between the surround's phase and the center's is very close to 180°

at the lowest temporal frequency and decreases to ~170° at 20 Hz; behavior is less uniform across cells above this temporal frequency.

It may help the reader to consider how the results of the decomposition explain the frequency responses measured with diffuse and peak stimuli. For the diffuse stimulus, the center and surround signals are of similar amplitude at low temporal frequencies and are nearly in anti-phase. A small net response results. At midrange temporal frequencies, the strengths of center and surround change little, but their signals cease to be exactly out of phase. The response to the diffuse stimulus therefore increases with temporal frequency. A temporal frequency is then reached at which the amplitude of the surround signal becomes substantially greater than that of the center and sometimes greater than that of both mechanisms at midrange frequencies. This is the origin of the maximum at

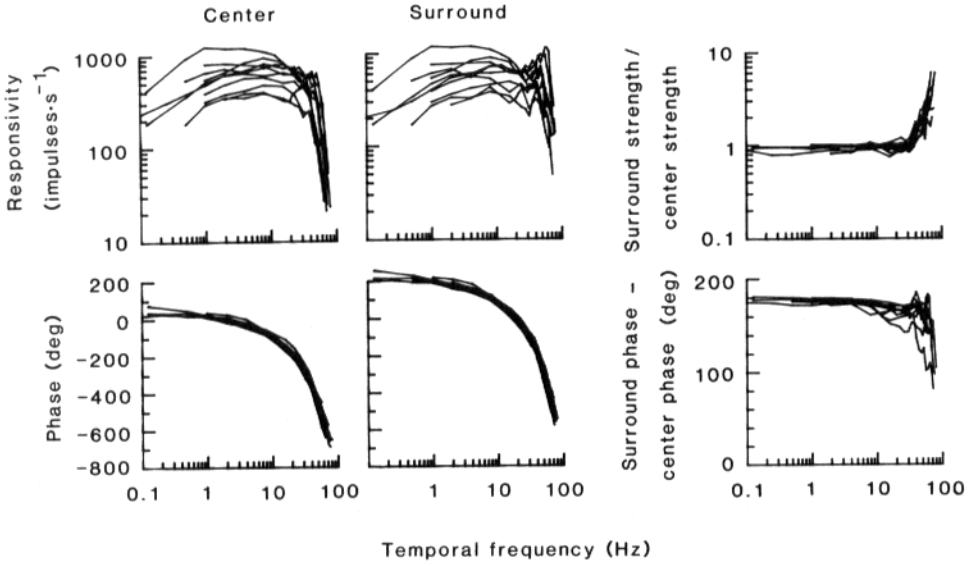

FIGURE 12. Photopic center and surround mechanism temporal frequency responses across X cells. This figure shows data similar to those in Fig. 12 for a total of 10 X cells.

high temporal frequency in the responsivity curve for the diffuse stimulus. This domination by the surround component at high temporal frequencies also explains the spatial frequency responses measured there (see Figs. 8 and 10). At low spatial frequency, the amplitude of the surround signal is dominant and the phase of the net response is close to that of the surround. As the spatial frequency increases past the spatial resolution of the surround mechanism, the magnitude of the net response drops correspondingly, and the phase swings toward that of the center signal.

DISCUSSION

This study provides a more complete description of the spatiotemporal frequency response of X ganglion cells than was previously available. New data on Y

ganglion cells at photopic levels and X cells at lower levels of retinal illumination are also reported. In the first part of the Discussion, retinal mechanisms that might underlie photopic spatiotemporal frequency responses are considered. In a later section, the relevance of our observations to vision is discussed, and finally, a possible model for the photopic spatiotemporal frequency response of X cells is described.

Mechanisms Underlying the Spatiotemporal Frequency Response

Frequency responses at low temporal frequencies. Two possible causes of the lower responsivities obtained for contrast modulation below 1 Hz are (*a*) light adaptation and (*b*) contrast gain control (Shapley and Victor, 1978). The roll-off on double-logarithmic axes has a fractional slope that becomes steeper as the cell is light-adapted from scotopic, through mesopic, to photopic illumination. There is some evidence that, within the scotopic range, the slope of the roll-off increases with mean illumination (Enroth-Cugell and Shapley, 1973). Any light-adaptational effect probably occurs early in the retina, since some attenuation at low temporal frequencies was found in horizontal cells in cat (Foerster et al., 1977*a*, *b*) and turtle (Tranchina et al., 1984).

The contrast gain control is also known to attenuate responses to low temporal frequencies of contrast modulation and to act more strongly in Y cells than in X cells. We found more attenuation in the Y cell responsivity than in that of X cells at low and midrange temporal frequencies. In addition, the attenuation observed for Y cells was stronger than that observed by previous investigators, whereas that for X cells was similar (e.g., Lennie, 1980; Derrington and Lennie, 1982). We may have seen more attenuation in Y cells because our average response criterion was higher by ~2 impulses·s^{-1} than the criteria used by Lennie (1980) and Derrington and Lennie (1982), and thus presumably required higher contrast and enhanced the contrast gain effect.

Frequency responses at high temporal frequencies. The enhanced responsivity at high temporal frequencies between 40 and 60 Hz was observed at photopic levels where rods were saturated, but not at mesopic or scotopic levels. This strongly suggests that the origin of the enhancement is in the "cone" pathway. Foerster et al. (1977*a*, *b*) found similar enhanced responses in cat horizontal cells under photopic conditions. Hence, the cellular origin of the enhancement of ganglion cell responsivity is probably early in the pathway.

One possibility may be a negative feedback loop in which cones excite horizontal cells and horizontal cells in turn inhibit cones, as is the case for the turtle retina (Baylor et al., 1971). If both cones and horizontal cells act as low-pass filters, then the complete loop could act as a second-order filter and produce a resonant peak, as suggested by Foerster et al. This feedback might also account for the greater enhancement of responses seen in cat horizontal cells (Foerster et al., 1977*a*, *b*) and in our ganglion cells for large stimuli.

A contributing factor to the response enhancement may be the reduced antagonism between center and surround signals that would occur if the two mechanisms were more nearly coherent at high temporal frequencies. A similar mechanism for the amplification of signals was described for *Limulus* eye by Ratliff et al. (1970). However, the fact, according to our decompositions, that

the responsivity of the surround surpasses that of the center and that both signals are rapidly attenuated at high temporal frequencies where the center and surround are most coherent implies that changes in signal amplitude are at least as important in describing the cell's peak in responsivity. In fact, the decompositions of photopic frequency responses show that the phases of the surround and center were still separated by >120° where responsivity peaked.

The roll-off at high temporal frequencies. The roll-off of responsivity of ~7 log units for each log unit of temporal frequency agrees well with the horizontal cell data of Foerster et al. (1977*a*), who found log-log gradients of about −6 for their medium-bandwidth cells and up to −7 for their wide-bandwidth cells. This suggests that the retinal elements that determine the high-frequency roll-off are cones or horizontal cells. There is evidence from other species of qualitatively similar low-pass filtering by receptors (e.g., Fuortes and Hodgkin, 1964; Baylor et al., 1974) and at the receptor bipolar synapse (Ashmore and Copenhagen, 1980).

Spatiotemporal resolution. We found a trade-off between spatial and temporal resolution; when one improved, the other deteriorated. First, as the 2-Hz center radius increased across our sample of cells, temporal resolution improved (Fig. 5). Second, in individual (on-center) X cells, increasing the temporal frequency above 32 Hz resulted in larger center radii (Fig. 9), an example of spatiotemporal interaction in the cells' receptive fields. Detwiler et al. (1978, 1980) found a similar trade-off in the network of turtle rods, as did Molenaar et al. (1983) in cone-driven responses of cat horizontal cells. The mechanism that Detwiler et al. proposed was inductance-like behavior in the receptor membrane, possibly caused by voltage-dependent membrane conductances. Such voltage-dependent conductances have been shown directly in the rods of toads (Torre and Owen, 1981) and salamander (Baylor et al., 1984).

In our experiments, temporal resolution increased for individual cells when we decreased the spatial frequency of the stimulus, and our decompositions indicated that the surround resolved higher temporal frequencies than the center. Maffei et al. (1970), on the other hand, concluded that it was the center and not the surround that determined the temporal resolution. However, they used spot stimuli, which may not have stimulated the surround mechanism as adequately as our gratings. Marcus (1979), on the other hand, used a stimulus more likely to generate a considerable surround signal and he found that the cell's response did increase at high temporal frequencies.

The high temporal resolutions at photopic levels for diffuse light that we observed have been reported previously for cat horizontal cells (Foerster et al., 1977*a*), and flicker fusions of up to 80 Hz also have been reported for retinal ganglion cells (Enroth, 1953; Ogawa et al., 1966). In addition, Jones and Berkeley (1983), who measured evoked potentials from the optic tract, dorsal lateral geniculate nucleus, and visual cortex, reported flicker resolutions of up to 90 Hz for large photopic spot stimuli.

Relation to Vision

Both X and Y cells respond poorly to low spatial frequencies at very low temporal frequencies (e.g., <1 Hz). In cats, the existing behavioral studies of contrast

sensitivity (Blake and Camisa, 1977; Loop and Berkeley, 1975) provide insufficient data to address this issue. However, it has been known for a long time that the combination of low spatial and temporal frequencies in humans leads to very poor contrast sensitivity (Robson, 1966; Kelly, 1974).

The responsivities for X and Y cells measured with the peak stimulus at photopic levels, and for X cells at mesopic levels, were optimal at ~5 or 6 Hz. A similar result was found under comparable stimulus conditions by previous investigators (Lennie, 1980; Derrington and Lennie, 1982), and this result does not appear to be altered a great deal at the dorsal lateral geniculate nucleus (Troy, 1983) or in areas 17 and 18 of the visual cortex (Movshon et al., 1978). Further, the optimal temporal frequencies observed in Blake and Camisa's (1977) behavioral study under high mesopic conditions were also similar.

With respect to temporal resolution in behavioral studies on cat, Loop and Berkeley (1975) found that, for a 15° patch of light, contrast sensitivity dropped to a value of unity at ~50 Hz, and extrapolations of Blake and Camisa's (1977) temporal contrast sensitivity curves for spatial frequencies of 0.25 and 0.5 cycles·deg^{-1} yield similar results. Our most appropriate data for comparison are the resolutions measured with diffuse stimuli at midmesopic adaptation levels. Under these circumstances, on average, X cells had temporal resolutions of ~53 Hz. While this comparison is necessarily a rough one (including the assumption that our X cell data cover the same retinal eccentricities used by the animal for performing the task), it suggests that, for spatially uniform fields, temporal resolution might be preserved from the retina up to the point where flicker detection occurs in cats.

Our findings, based on X cells, show that for all three spatial stimuli, temporal resolution increases slightly with center radius (Fig. 5) and hence with retinal eccentricity (e.g., Cleland and Levick, 1974; Stone and Fukuda, 1974; Cleland et al., 1979). We know of no behavioral data for the cat that test this issue, but in psychophysical studies in humans, Kelly (1984) found that within the central 12°, the temporal frequency contrast sensitivity does not depend on eccentricity, provided that it is measured with the optimal spatial frequency for that eccentricity; this is in agreement with previous findings by Virsu et al. (1982). This issue clearly needs to be studied in cats.

Modeling the Temporal Frequency Response

Center-surround decomposition. Consistent results were obtained in three previous studies in which X cell spatial frequency responses were measured at more than one temporal frequency and were analyzed using the difference-of-Gaussians or the Gaussian center-surround model. In the temporal frequency ranges modeled—0.16–20.4 Hz for Derrington and Lennie (1982), 0.5–32 Hz for Enroth-Cugell et al. (1983), and 1–16 Hz for Dawis et al. (1984)—center and surround radii showed no consistent change with temporal frequency. Enroth-Cugell et al. (1983) also showed that the ratio of center and surround strength is a flat function of temporal frequency over the frequency range that they studied. Further, the surround-center phase difference decreased on average by ~30°. We also found that the ratio of surround to center strength changed little up to ~30 Hz, and that the phase difference between mechanisms

decreased by between ~10° and 40° at that frequency. Thus, up to ~30 Hz, our data would be fitted adequately by the existing Gaussian center-surround model (e.g., Enroth-Cugell et al., 1983). It was our findings past this frequency that led us to apply a more general model in which the center and surround radii are allowed to vary with temporal frequency.

A model for the temporal frequency response. Assuming that the X cell receptive field is adequately described by the Gaussian center-surround model, the temporal frequency response of an X cell can be quantitatively modeled by finding

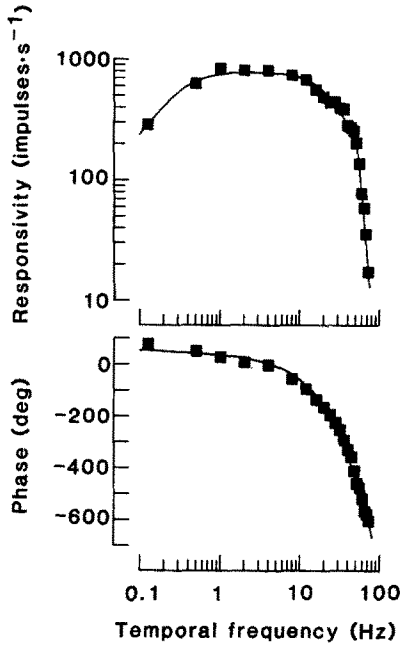

FIGURE 13. Fit of a model with six first-order low-pass filters, one second-order filter, a transitional lead, and a time delay to the temporal photopic frequency response measured with the peak stimulus for the unit (13X8) that was featured in Figs. 1, 8, and 10. For this particular cell, the corner frequencies for the six low-pass filters were at 46 Hz and the corner frequency for the second-order filter was at 53 Hz. The second-order filter had a damping constant of 0.17. The parameters g and τ of the transitional lead were 9 and 4 s, respectively. The time delay was 15 ms and the overall gain was 800 impulses·s^{-1}.

two linear systems, one that emulates the center mechanism's temporal frequency response and another that emulates that of the surround. The shape of the center's temporal frequency response above 1 Hz suggests a cascade of about six first-order low-pass filters and one second-order filter (the second-order filter being added to fit the slight enhancement at 40–50 Hz). The surround's temporal frequency response, which is more enhanced than the center's at 40–50 Hz, requires a lower damping constant for the second-order filter. The surround's

model has an additional short delay of a few milliseconds (Enroth-Cugell et al., 1983), but is otherwise similar to that of the center. As the frequency decreases below 1 Hz, the use of the low-pass filters alone would require that both the center and surround strengths (i.e., responsivities at zero spatial frequency) approach a constant value, and that the center phase approach 0° and the surround phase 180° for an on-center cell. In fact, the strengths of both models decrease at the rate of ~0.5 log unit per log unit of temporal frequency and their phases are advanced by ~40° over the above values. To account for these observations, an additional element has to be added to both the center and surround pathways; a suitable choice, suggested by Dr. J. G. Robson, would be a transitional lead (an element with frequency response $[1 + (i\tau 2\pi w)/(g + i\tau 2\pi w)]$, where τ is a time constant, w is temporal frequency, and g is a constant >1). With all these elements, the model still does not account for the change in the response phase that occurs over the temporal frequency range that we studied, which suggests that there is another component in both pathways that produces a phase delay without observable amplitude attenuation: a pure delay of ~10–15 ms (or, equivalently, a cascade of low-pass filters with very high corner frequencies) is a candidate for this component. A pure delay could arise from synaptic and transport delays; a delay of 3–4 ms might be due to the fact that the site of recording was mainly in the optic tract in these experiments.

The adequacy of our model for the center signal, complete with six first-order low-pass filters, one second-order filter, a transitional lead, and a pure delay, is illustrated in Fig. 13, where it is fitted to a photopic temporal frequency response of an X cell stimulated with the peak spatial frequency. The closeness of the fit brings us to the conclusion that a model of the general form described above can predict our spatiotemporal frequency response measurements. That such a complex form of model is needed doubtless reflects the sophisticated signal processing undertaken by the neurons in the retina.

We are grateful to Dr. John Robson for sharing his observations with us.

This work was supported by National Eye Institute (NEI) grant R01 EY00206 to C.E.-C., NEI New Investigator Award 5 R23 EY03738 to D.S.T., and NEI Postdoctoral Fellowship F32EY05297 to L.J.F. A.W.F. was supported by grant F05 TW03177 from the Fogarty Center of the National Institutes of Health, and J.B.T. was supported by NATO/SERC grant B/RF/5881 and National Science Foundation grant BNS 82-13858.

Original version received 21 May 1986 and accepted version received 27 October 1986.

REFERENCES

Ashmore, J. F., and D. R. Copenhagen. 1980. Different postsynaptic events in two types of retinal bipolar cell. *Nature.* 288:84–86.

Baylor, D. A., M. G. F. Fuortes, and P. M. O'Bryan. 1971. Receptive fields of cones in the retina of the turtle. *Journal of Physiology.* 214:265–294.

Baylor, D. A., A. L. Hodgkin, and T. D. Lamb. 1974. Reconstruction of the electrical responses of turtle cones to flashes and steps of light. *Journal of Physiology.* 242:759–791.

Baylor, D. A., G. Matthews, and B. J. Nunn. 1984. Location and function of voltage sensitive

conductances in retinal rods of the salamander *Ambystoma tigrinum*. *Journal of Physiology*. 354:203–233.

Blake, R., and J. M. Camisa. 1977. Temporal aspects of spatial vision in the cat. *Experimental Brain Research*. 28:325–333.

Cleland, B. G., T. H. Harding, and U. Tulunay-Keesey. 1979. Visual resolution and receptive field size: examination of two kinds of retinal ganglion cell. *Science*. 205:1015–1017.

Cleland, B. G., and W. R. Levick. 1974. Brisk and sluggish concentrically organized ganglion cells in the cat's retina. *Journal of Physiology*. 240:421–456.

Dawis, S., R. Shapley, E. Kaplan, and D. Tranchina. 1984. The receptive field organization of X-cells in the cat: spatiotemporal coupling and asymmetry. *Vision Research*. 24:549–564.

Derrington, A. M., and P. Lennie. 1982. The influence of temporal frequency and adaptation level on receptive field organization on retinal ganglion cells in cat. *Journal of Physiology*. 333:343–366.

Detwiler, P. B., A. L. Hodgkin, and P. A. McNaughton. 1978. A surprising property of electrical spread in the network of rods in the turtle's retina. *Nature*. 274:562–565.

Detwiler, P. B., A. L. Hodgkin, and P. A. McNaughton. 1980. Temporal and spatial characteristics of the voltage response of rods in the retina of the snapping turtle. *Journal of Physiology*. 300:213–250.

Enroth, C. 1953. Spike frequency and flicker fusion frequency in retinal ganglion cells. *Acta Physiologica Scandinavica*. 29:19–21.

Enroth-Cugell, C., T. K. Goldstick, and R. A. Linsenmeier. 1980. The contrast sensitivity of cat retinal ganglion cells at reduced oxygen tensions. *Journal of Physiology*. 304:59–81.

Enroth-Cugell, C., B. G. Hertz, and P. Lennie. 1977. Cone signals in the cat's retina. *Journal of Physiology*. 269:273–296.

Enroth-Cugell, C., and J. G. Robson. 1966. The contrast sensitivity of retinal ganglion cells of the cat. *Journal of Physiology*. 187:517–552.

Enroth-Cugell, C., J. G. Robson, D. E. Schweitzer-Tong, and A. B. Watson. 1983. Spatio-temporal interactions in cat retinal ganglion cells showing linear spatial summation. *Journal of Physiology*. 341:279–307.

Enroth-Cugell, C., and R. M. Shapley. 1973. Adaptation and dynamics of cat retinal ganglion cells. *Journal of Physiology*. 233:271–309.

Foerster, M. H., W. A. van de Grind, and O.-J. Grusser. 1977*a*. Frequency transfer properties of three distinct types of cat horizontal cells. *Experimental Brain Research*. 29:347–366.

Foerster, M. H., W. A. van de Grind, and O.-J. Grusser. 1977*b*. The response of cat horizontal cells to flicker stimuli of different area, intensity and frequency. *Experimental Brain Research*. 29:367–385.

Fuortes, M. G. F., and A. L. Hodgkin. 1964. Changes in time scale and sensitivity in the ommatidia of *Limulus*. *Journal of Physiology*. 172:239–263.

Hochstein, S., and R. M. Shapley. 1976. Quantitative analysis of retinal ganglion cell classifications. *Journal of Physiology*. 262:237–264.

Jones, K. R., and M. A. Berkley. 1983. Loss of temporal sensitivity in dorsal lateral geniculate nucleus and area 18 of the cat following monocular deprivation. *Journal of Neurophysiology*. 49:254–268.

Kaplan, E., S. Marcus, and Y. T. So. 1979. Effects of dark adaptation on spatial and temporal properties of receptive fields in cat lateral geniculate nucleus. *Journal of Physiology*. 294:561–580.

Kelly, D. H. 1974. Spatio-temporal frequency characteristics of colour-vision mechanisms. *Journal of the Optical Society of America*. 64:983–990.

Kelly, D. H. 1984. Retinal inhomogeneity. I. Spatiotemporal contrast sensitivity. *Journal of the Optical Society of America.* A1:107–113.

Kirby, A. W., and D. E. Schweitzer-Tong. 1981. GABA-antagonists alter spatial summation in receptive field centres of rod- but not cone-driven cat retinal ganglion Y-cells. *Journal of Physiology.* 320:303–308.

Lederer, W. J., A. J. Spindler, and D. A. Eisner. 1979. Thick slurry bevelling: a new technique for bevelling extremely fine microelectrodes and micropipettes. *Pflügers Archiv.* 381:287–288.

Lennie, P. 1980. Perceptual signs of parallel pathways. *Philosophical Transactions of the Royal Society of London, Series B.* 290:23–37.

Levick, W. R. 1972. Another tungsten microelectrode. *Medical Biology and Engineering.* 10:510–515.

Linsenmeier, R. A., L. J. Frishman, H. G. Jakiela, and C. Enroth-Cugell. 1982. Receptive field properties of X and Y cells in the cat retina derived from contrast sensitivity measurements. *Vision Research.* 22:1173–1183.

Loop, M. S., and M. A. Berkley. 1975. Temporal modulation sensitivity of the cat. 1. Behavioral measures. *Vision Research.* 15:555–561.

Maffei, L., L. Cervetto, and A. Fiorentini. 1970. Transfer characteristics of excitation and inhibition in cat retinal ganglion cells. *Journal of Neurophysiology.* 33:276–284.

Marcus, S. 1979. Effects of contrast and spatial configuration upon the tuning characteristics of cat retinal and LGN cells. Ph.D. thesis. The Rockefeller University, New York. 222 pp.

Molenaar, J., W. A. Van de Grind, and R. Eckhorn. 1983. Dynamic properties of cat horizontal cell light responses. *Vision Research.* 23:257–266.

Movshon, J. A., I. D. Thompson, and D. J. Tolhurst. 1978. Spatial and temporal contrast sensitivity of neurons in areas 17 and 18 of the cat's visual cortex. *Journal of Physiology.* 283:101–120.

Ogawa, T., P. O. Bishop, and W. R. Levick. 1966. Temporal characteristics of responses to photic stimulation by single ganglion cells in the unopened eye of the cat. *Journal of Neurophysiology.* 29:1–30.

Pettigrew, J. D., M. L. Cooper, and G. G. Blasdel. 1979. Improved use of tapetal reflection for eye-position monitoring. *Investigative Ophthalmology and Visual Science.* 18:490–495.

Ratliff, F., B. W. Knight, and N. Milkman. 1970. Superposition of excitatory and inhibitory influences in the retina of *Limulus*: effect of delayed inhibition. *Proceedings of the National Academy of Sciences.* 67:1558–1564.

Robson, J. G. 1966. Spatial and temporal contrast sensitivity functions of the human visual system. *Journal of the Optical Society of America.* 56:1141–1142.

Rodieck, R. W. 1965. Quantitative analysis of cat retinal ganglion cell response to visual stimuli. *Vision Research.* 5:583–601.

Schweitzer-Tong, D. E. 1983. The photoneuromine: an artificial visual neuron for dynamic testing of computer-controlled experiments. *Behavioral Research Methods and Instrumentation.* 15:9–12.

Shapley, R. M., and J. D. Victor. 1978. The effect of contrast on the transfer properties of cat retinal ganglion cells. *Journal of Physiology.* 285:275–298.

So, Y. T., and R. Shapley. 1981. Spatial tuning of cells in and around the lateral geniculate nucleus of the cat: X and Y relay cells and perigeniculate interneurons. *Journal of Neurophysiology.* 45:107–120.

Stone, J., and Y. T. Fukuda. 1974. Properties of cat retinal ganglion cells: a comparison of W-cells with X- and Y-cells. *Journal of Neurophysiology.* 37:722–748.

Torre, V., and W. G. Owen. 1981. Ionic basis of high-pass filtering of small signals by the network of retinal rods in the toad. *Proceedings of the Royal Society of London, Series B.* 212:253–261.

Tranchina, D., J. Gordon, and R. M. Shapley. 1984. Retinal light adaptation: evidence for a feedback mechanism. *Nature.* 310:314–316.

Troy, J. B. 1983. Spatio-temporal interaction in neurones of the cat's dorsal lateral geniculate nucleus. *Journal of Physiology.* 344:419–432.

Virsu, V., J. Rovamo, P. Laurinen, and R. Nasanen. 1982. Temporal contrast sensitivity and cortical magnification. *Vision Research.* 22:1211–1217.